

Form birefringence of air guiding photonic crystal fibers

Marcin Szpulak¹, Rafal Kotynski², Tomasz Nasiłowski², Wacław Urbańczyk¹, and Hugo Thienpont²

¹Wrocław University of Technology, 50-370 Wrocław, Wybrzeże Wyspiańskiego 27, Poland

²Department of Applied Physics and Photonics, Vrije Univ. Brussel, Pleinlaan 2, B-1050 Brussel

The paper presents a theoretical comparison of air guiding photonic crystal fibers with hexagonal lattice in terms of modal birefringence. Our modeling is fully vectorial and combines a plane-wave approach for bandgap determination with modal analysis based on the finite element method. We estimate the amount of form birefringence induced in the PCF when the symmetry of the structure is released either by a perturbation of the lattice itself, or by the anisotropy of the core shape.

Introduction

In recent years, photonic crystal fibers (PCFs) [1] have been the subject of extensive research. It has been already demonstrated that PCF can be used in numerous applications including chromatic dispersion compensation [2], supercontinuum generation [3], construction of novel fiber lasers [4] and many other. Particularly interesting are the polarization properties of PCFs. It is already well known [5,6] that modal birefringence of PCFs may exceed 10^{-3} , which is by one order of magnitude higher than the birefringence in classical Hi-Bi fibers. It has been also shown that PCF can operate in a single-polarization regime and can be used as wide-band fiber polarizers [7].

There are only a few papers published so far related to highly birefringent photonic bandgap fibers (HiBi-PBGF) [8, 9]. Here, we propose and analyze two novel designs of HiBi-PBGF. The first structure is presented in Fig. 1a. It is based on the hexagonal lattice with the pitch of $\Lambda=2 \mu\text{m}$, with circular holes of diameter d , and with the filling fraction equal to $d/\Lambda=0.9$. Birefringence in this structure is caused by the elliptical shape of the core.

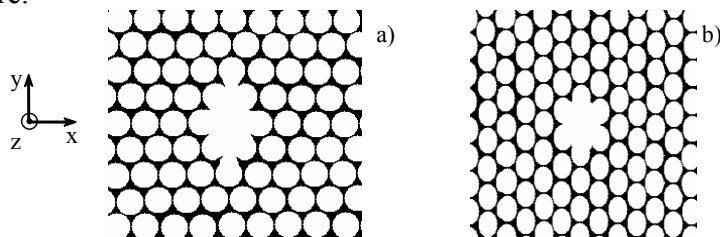


Fig 1. Cross-section of the PCF: **a)** based on the hexagonal lattice with the elliptical shape of the core; **b)** based on the squeezed hexagonal lattice.

The second structure (Fig. 1b) is based on exactly the same lattice, squeezed in one dimension by the factor of 0.75. In this case, birefringence results from the C_{2v} symmetry, which characterizes the lattice, the elliptical holes, as well as the core.

In order to avoid the appearance of surface modes, the PCFs shown in Fig. 1 have been designed in such a way that their core boundaries intersect the claddings in areas where the widths of the silica glass layers are the thinnest [10].

Photonic bandgap computations

We have determined the photonic bandgap (PBG) structures of the PCF claddings by solving numerically the vectorial wave eigenequation for the transverse magnetic fields and propagation constants. In these calculations we have used the plane wave method [11], with 63x63 plane waves.

For the hexagonal lattice of the PCF from Fig. 1a, the light-line lies inside the bandgap between 1.3 μm and 1.46 μm . In Fig. 2, we have plotted the more interesting PBG structure of the squeezed lattice from Fig. 1b. Due to the C_{2V} symmetry, the bandgaps for each polarization are different, and we plot them separately (Fig 2a-d). The shifted bandgap for the Y-polarization may be connected to the contraction of the lattice in the orthogonal direction. The differences between the PBG structures obtained for the two energy threshold levels (Fig. 2) indicate a hybrid character of the plotted modes.

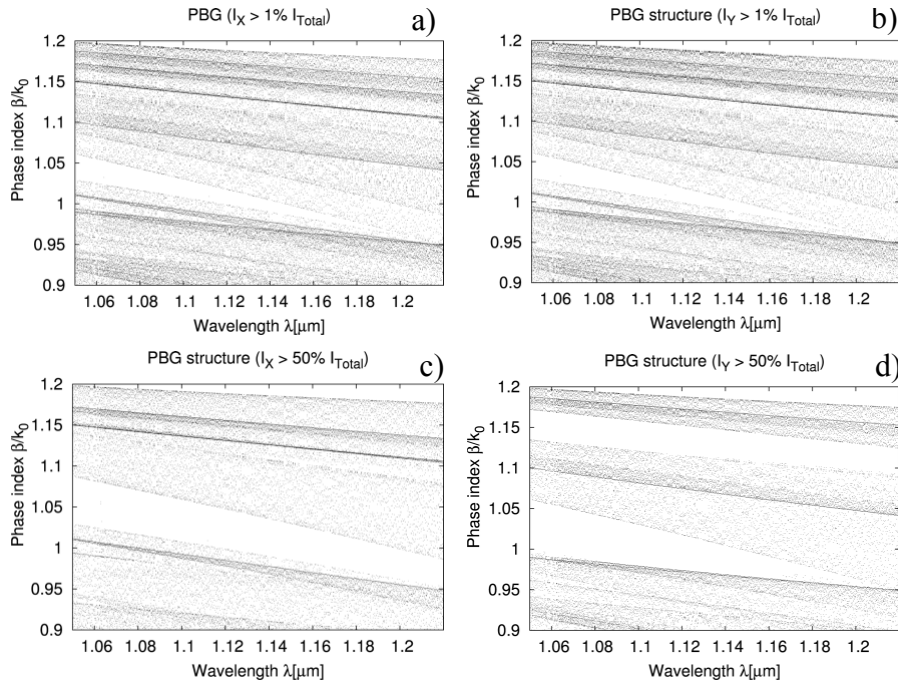


Fig. 2. The photonic bandgap of the squeezed air-silica lattice from Fig 1.b. vs. wavelength. The plotted modes contain **a)** over 1% of energy in the X-polarization; **b)** over 1% of energy in the Y-polarization; **c)** over 50% of energy in the X-polarization; **d)** over 50% of energy in the Y-polarization.

Phase and group birefringence

In Fig. 3 we present the wavelength dependence of the birefringence for the two analyzed PCF designs. We have calculated both the phase birefringence $B(\lambda)$ and the group birefringence $G(\lambda)$, defined as:

$$B = \frac{\lambda}{2\pi} (\beta_y - \beta_x), \quad (1)$$

and

$$G = B - \lambda \frac{dB}{d\lambda}, \quad (2)$$

respectively. In Eq. (1), β_x and β_y denote the propagation constants of the two orthogonally polarized fundamental air-guided modes. Our modal calculations are based on the the fully vectorial wave equation that we solve using the finite element method [12] with hybrid edge/nodal triangular elements. The mesh used in calculations consists of around 50000 elements and covers a single quadrant of the PCF cross-profile.

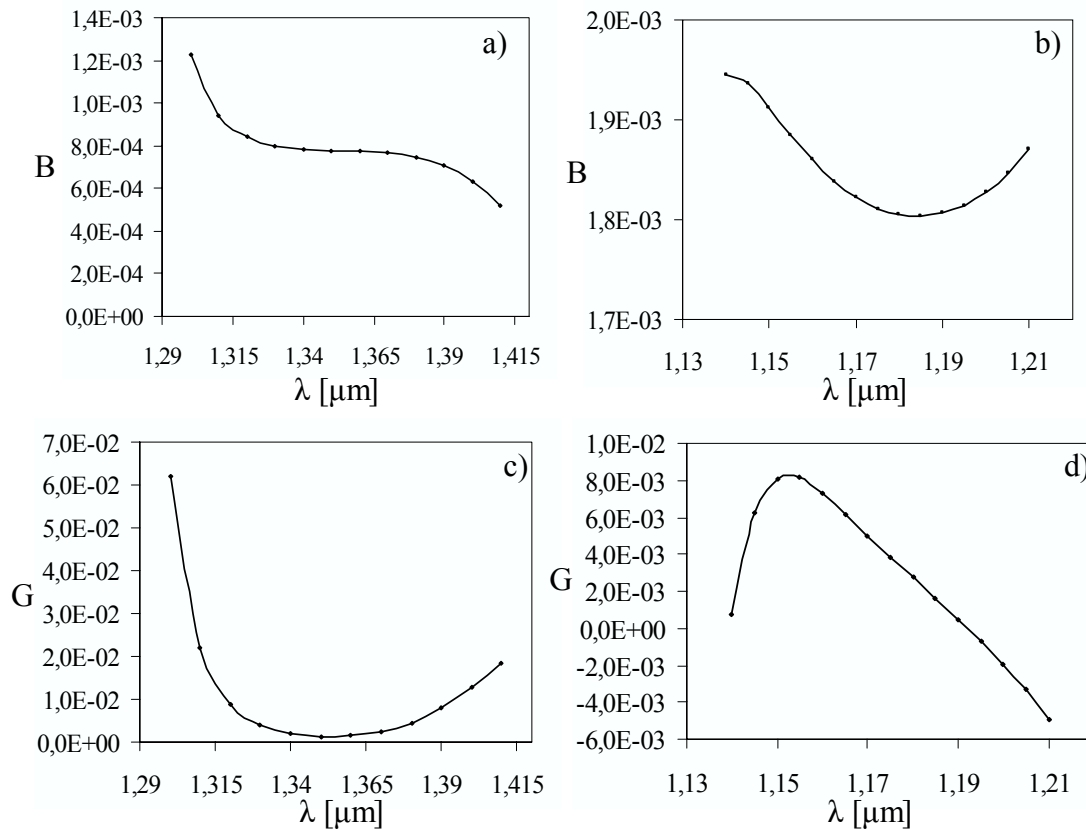


Fig. 3 Phase birefringence B , and group birefringence G in the function of wavelength. **a)** B for the PCF from Fig. 1a; **b)** B for the PCF from Fig. 1b; **c)** G for the PCF from Fig. 1a; **d)** G for the PCF from Fig. 1b.

As we see from Fig.3a, the phase birefringence $B(\lambda)$ of the PCF from Fig.1a varies between $1.3 \cdot 10^{-3}$ and $5 \cdot 10^{-4}$, and is monotonically decreasing. $B(\lambda)$ is strongly dispersive near the band edges, and relatively flat with $B \approx 8e-4$ around the middle of the band. Since $dB/d\lambda < 0$, the group birefringence G is positive (Fig. 3c), and reaches $6 \cdot 10^{-2}$ at the short wavelength edge of the bandgap. The phase birefringence of the second PCF from Fig. 1b, varies between $1.95 \cdot 10^{-3}$ and $1.8 \cdot 10^{-3}$ with the minimum at the wavelength of $1.185 \mu\text{m}$ (Fig.3b). The smaller dispersion of B for this structure causes the group birefringence G to be smaller, with the maximal value of $8 \cdot 10^{-3}$ at the wavelength of $1.15 \mu\text{m}$. The existence of an extremum of $B(\lambda)$ causes the group birefringence G (Fig.3d) to change its sign at the wavelength of $1.19 \mu\text{m}$.

In Fig. 4 we present the field distributions of the Y-polarized fundamental mode for the two HiBi-PBG fibers shown on Fig.1.a and Fig.1.b, calculated at the wavelengths of $1.3 \mu\text{m}$ and $1.13 \mu\text{m}$ respectively. Both wavelengths are situated at the edge of the bandgap, thus the modal field penetrates deeply into the cladding and is highly hybridized.

Conclusions

We have proposed and analyzed two designs of highly birefringent photonic bandgap fibers. We have shown that in both cases, the phase birefringence is of the order of 10^{-3} and is highly dispersive, while group birefringence may reach the order of 10^{-2} . Moreover in case of the fiber with elliptical holes, the group birefringence undergoes a change of sign.

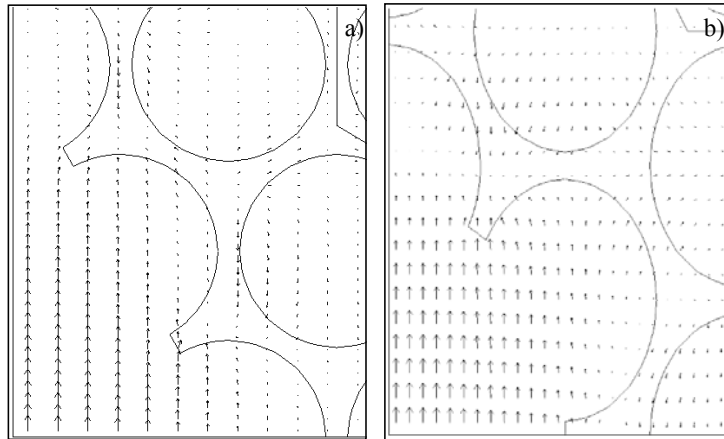


Fig. 4. Electric field distribution of the Y-polarized mode calculated over one quarter of the fiber's cross-section: **a)** for the PCF from Fig. 1a, at $1.3\mu\text{m}$; **b)** for the PCF from Fig. 1b at $1.13\mu\text{m}$.

Acknowledgements

We acknowledge financial support from the Polish Committee for Scientific Research, Grant No. 4 T10C 035 24, the Bilateral Agreement between Poland and Flanders BOF-BWS 2003, and the EC 6th FP Network of Excellence on Micro-Optics "Nemo".

References

- [1] T. A. Birks, J. C. Knight, P. St. J. Russel, *Opt. Lett.* **22**, 961-963 (1997).
- [2] F. Poli, A. Cucinotta, M. Fuocho, S. Selleri, L. Vincenzia, *J. Opt. Soc. Am A* **20**, 1958-1962 (2003).
- [3] W. J. Wadsworth, A. Ortigosa-Blanch, J. C. Knight, T. A. Birks, T.P. Martin Man, P. St. J. Russell, *J. Opt. Soc. Am. B* **19**, 2148-2155 (2002).
- [4] J. Limpert, T. Schreiber, S. Nolte, H. Zellmer, T. Tunnermann, R. Iliew, and F. Lederer, J. Broeng, G. Vienne, A. Petersson, and C. Jakobsen, *Opt. Express* **11**, 818-823 (2003).
- [5] A. Ortigosa-Blanch, J.C. Knight, W.J. Wadsworth, J. Arriaga, B.J. Mangan, T. A. Birks, P. St. J. Russell, *Opt. Lett.* **25**, 1325-1327 (2000).
- [6] T.P.Hansen, J. Broeng, S.E.B. Libori, E.Knudsen, A.Bjarklev, J.R.Jensen, H.Simonsen, *IEEE Photon. Tech. Lett.* **13**, 588-590 (2001).
- [7] K. Saitoh, M. Koshiha, *Photon. Technol. Lett.* **15**, 1384-1386 (2003).
- [8] K. Saitoh, M. Koshiha, *IEEE Photon. Tech. Lett.* **14**, 1291-1293 (2002).
- [9] X.Chen et al, *Opt. Express* **12**, 3888-2893 (2004).
- [10] M.J.F.Digonnet, H.K.Kim, J.Shin, S.Fan, G.S.Kino, *Opt. Express* **12**, 1864-1872 (2004).
- [11] T.A.Birks, D.M.Bird, T.D.Hedley, J.M.Pottage, P.St.J.Russell, *Opt. Express*, **11**, 2854-2861 (2003).
- [12] M. Koshiha, K. Saitoh, *Applied Optics* **42** 6267-6275 (2003).